



Trade Science Inc.

ISSN : 0974 - 7486

Volume 7 Issue 4

# Materials Science

An Indian Journal

Full Paper

MSAIJ, 7(4), 2011 [250-255]

## Photoelectrocatalytic hydrolysis of starch by sprayed ZnO thin film

R.T.Sapkal<sup>1</sup>, S.S.Shinde<sup>1</sup>, M.R.Sapkal<sup>2</sup>, A.R.Babar<sup>1</sup>, D.M.Sapkal<sup>1</sup>, C.B.Jalkute<sup>4</sup>,  
K.Y.Rajpure<sup>1</sup>, P.S.Patil<sup>3</sup>, K.D.Sonawane<sup>4</sup>, C.H.Bhosale<sup>1\*</sup>

<sup>1</sup>Electrochemical Materials Laboratory, Department of Physics, Shivaji University, Kolhapur - 416 004, (INDIA)

<sup>2</sup>Department of Microbiology, B. D. College, Patan, Dist-Satara - 415 102, (INDIA)

<sup>3</sup>Thin Film Materials Laboratory, Department of Physics, Shivaji University, Kolhapur - 416 004, (INDIA)

<sup>4</sup>Department of Microbiology, Shivaji University, Kolhapur - 416 004, (INDIA)

E-mail : bhosale\_ch@yahoo.com

Received: 19<sup>th</sup> January, 2011 ; Accepted: 29<sup>th</sup> January, 2011

### ABSTRACT

Zinc oxide (ZnO) thin films of different thickness have been deposited onto glass/FTO substrates by spray pyrolysis method. The films were characterized by XRD, optical transmittance, Reflectance and SEM techniques. All the films are polycrystalline with hexagonal wurtzite structure, with c- axis growth (002) perpendicular to substrate surface. Starch was hydrolyzed by novel Photoelectrocatalytic process. Hydrolyzed starch was found to contain 60 $\mu\text{g ml}^{-1}$  of glucose and 100 $\mu\text{g ml}^{-1}$  of maltose. © 2011 Trade Science Inc. - INDIA

### INTRODUCTION

Heterogeneous photocatalysis on semiconductor surfaces has attracted a lot of attention due to important applications like water disinfection, degradation and complete mineralization of organic contaminants in wastewater, air purification and water splitting for hydrogen production<sup>[1]</sup>. Zinc oxide (ZnO) is a transparent direct wide band-gap semiconductor ( $E_g = 3. \text{ eV}$ ) with a large exciton binding energy, which has been comprehensively studied due to its outstanding properties including piezoelectricity, n-type conductivity and room temperature (RT) ferromagnetism upon appropriate doping, great chemical sensing effects and remarkable photocatalytic activity<sup>[2]</sup>. Besides, it has been reported that ZnO shows better activity than TiO<sub>2</sub> in the photodegradation of some dyes in aqueous solutions since it can absorb more light quanta<sup>[3]</sup>. Recent studies have focused on the deposition of photoactive TiO<sub>2</sub>

thin films on glass substrates<sup>[4,5]</sup>. However, only few reports on the photocatalytic properties of nanostructured ZnO thin films<sup>[6,7]</sup>. Moreover, to our knowledge, there has been no systematic study investigating the dependence of the photocatalytic activity of ZnO thin films and nanostructures synthesized by chemical methods on film crystallinity, morphology and thickness.

Starch is widely used in various branches of industry not only for preparing gel-like accessory (thickening, gluing, binding, finishing, etc.) materials, but also as environmentally safe precursor of new preparations. When gel-like materials are prepared from starch products, it is necessary to break down its primary structure formed by swollen starch granules, and when starch is used as a precursor for organic and enzymatic synthesis, its preliminary depolymerization (liquation) is required. Mechanical degradation of gelatinized starch upon hydroacoustic treatment in a rotary pulse installation was studied by spectrophotometry of the iodine-

starch complexes and analysis of the concentrations of the terminal reducing groups. The energy efficiency of hydroacoustic and ultrasonic mechanical degradation was estimated<sup>[8]</sup>. The effect of starch concentration, temperature, time and enzyme concentration were studied and optimized for hydrolysis of corn flour starch powder (of mesh size 80/120) into glucose syrup by immobilized (using sodium alginate)  $\alpha$ -amylase using central composite design.<sup>[9]</sup>

The action of hydrogen peroxide and ferrous sulfate upon starch is a hydrolysis, producing in the course of the reaction dextrans, sugars of high molecular weight, and simple sugars<sup>[10]</sup>. Many researches have paid attention on hydrolysis by different methods<sup>[11-13]</sup>. Most industrial processes use enzymes to hydrolysis starch to high DE glucose syrups, usually in a two-step process: liquefaction and saccharification, which lengthy and costly compared to photoelectrocatalytic hydrolysis of starch.

In the present investigation, ZnO films of different thickness were deposited at substrate temperature 400 °C by spray pyrolysis, using an aqueous mixture. The effect of film thickness on the film properties, like crystal structure, surface morphology, resistivity and optical properties were studied. The optimized ZnO electrode used for photoelectrocatalytic hydrolysis of starch.

## EXPERIMENTAL

ZnO thin films were deposited by a locally made spray pyrolysis deposition chamber on to glass substrate (75 X 25 X 2 mm<sup>3</sup>) using zinc acetate ( $\text{Zn}(\text{CH}_3\text{COO})_2 \cdot 2\text{H}_2\text{O}$ ) as precursor. The solution of zinc acetate was prepared in water + methanol + acetic acid (25 + 65 + 10)<sup>[14]</sup>. The films were prepared by varying the quantity of sprayed solution at optimized deposition temperature 400°C and 0.2M concentration of zinc acetate in order to optimize quantity of sprayed solution. Other parameters such as spray rate (5cc min<sup>-1</sup>), nozzle to substrate distance (33 cm) and carrier air pressure (2 atm) were kept at their fixed value throughout deposition process. Glass substrates were ultrasonically cleaned by deionized water, acetone and methanol before the experiment. The structural properties were studied by Philips X-ray diffractometer PW-1710 (= 1.5405 Å) using Cu - K $\alpha$  radiation in the span of 20 to 80°. Surface morphology of the thin film

was studied with JEOL JSM-6360 Scanning Electron Microscope (SEM). Optical absorption study was carried out in the wavelength range 300 - 1000 nm using spectrometer Systronic model -119. Resistivity was measured with two probe setup. Then ZnO thin film was deposited on glass/FTO substrate (100 X 100 X 2 mm<sup>3</sup>) at optimized parameters.

For photoelectrocatalytic hydrolysis of starch, 1% starch solution was prepared by dissolving 1 gm of starch powder into 100 cc distilled water. The prepared starch solution was recirculated through specially designed photoelectrocatalytic reactor at constant flow rate 12.2 lit/h. After suitable interval of time, 10 ml starch was taken out to study photocatalytic hydrolysis response of ZnO thin film. Optical absorption study of iodine-starch complex was carried out in the wavelength range 300 - 1000 nm using spectrometer Systronic model -119. Collected residue was examined by Raman spectroscopy and compared to untreated starch. To determine the hydrolysis of starch, collected solution was checked for the presence of maltose and glucose by DNSA method.

## RESULTS AND DISCUSSION

### Characterization of ZnO thin film

The as-grown films were characterized by XRD using Cu-K $\alpha$  radiation. The XRD patterns obtained for the films grown on glass substrates were studied in the 2 $\theta$  range of 20-100°. XRD pattern shown in Figure 1 shows that the material deposited is polycrystalline irrespective to the quantity of spraying solution. The observed d-values are matching to the standard d-values, which confirms that the films exhibit hexagonal (Wurtzite) crystal structure with preferential growth along the (002) plane. The lattice parameter values are in good agreement with the standard data<sup>[15]</sup>. The XRD pattern of the films shows that the preferred orientation of the films depend on its thickness. For example, the films having a thickness of the order 790 nm for 100 cc of spraying solution are more oriented than others. The variation of preferred orientation with respect to quantity of spraying solution may also be attributed to the variation in the film thickness. The film thickness effect on the peak intensity in the XRD pattern has been reported<sup>[16]</sup>. Above 200 cc, milky and powdery films were resulted.

## Full Paper

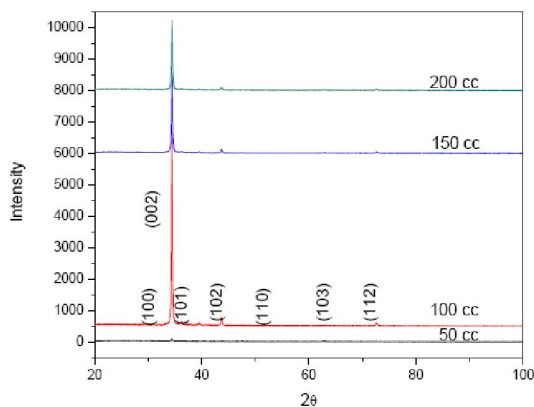


**Figure 1 : XRD patterns of ZnO thin films deposited using 0.2 M concentration at different temperatures**

All the peaks in the diffraction pattern were indexed on the basis of a JCPDS data card 05 - 6044. The crystallite size of the ZnO thin films was evaluated from the full width at half maxima (FWHM) of (002) peak using Scherrer's formula,

$$D = \frac{0.94\lambda}{\beta \cos \theta} \quad (1)$$

Where  $\lambda$ ,  $\theta$  and  $\beta$  are X-ray wavelength, Bragg diffraction angle and FWHM respectively.

The crystallite size lies within 38 - 52 nm range. The slight decreases in crystallite size after 400°C might be due to increases in film thickness. Quantitative information concerning the preferential crystal orientation can be obtained from the texture coefficient, TC defined as,

$$TC(hkl) = \frac{I(hkl)}{I_0(hkl)} \quad (2)$$

$$\frac{1}{n} \sum \frac{I(hkl)}{I_0(hkl)}$$

Where TC (hkl) is the texture coefficient, I (hkl) is the XRD intensity and n is number of diffraction peaks considered,  $I_0$  (hkl) is the intensity of the XRD reference of randomly oriented grains.

If  $TC(002) \approx 1$  for all hkl planes considered, then the films are with randomly oriented crystallite, while values higher than 1 indicate the abundance of grains in a given (hkl) direction. The values  $0 < TC(hkl) < 1$  indicates the lack of grains oriented in that direction. As TC (hkl) increase, the preferential growth of the crystallites in the direction perpendicular to the hkl plane is the higher. TC (002) is relatively higher at 100 ml.

The surface topology of the synthesized ZnO rods examined by the SEM is shown in figure 2. These SEM

images show that, rods becomes regular and almost perpendicular to the substrate, indicating that ZnO rods preferentially grow along the (002) direction. Optical transmission and reflection spectra of ZnO rods are shown in figure 3 and figure 4 respectively. The films are uniform and transparent. This is also confirmed by the transmittance and reflectance spectra of the films. The developed interference pattern in the transmittance shows that the films are specular to a great extent and high transmittance for the film deposited at 100 ml, as solution quantity increases transmittance goes on decreasing, which confirms the increase in thickness (TABLE 1). The average transmittance of the films in the visible region is about 95 %, which is higher than pervious works reported over 90%<sup>[17]</sup>. Thickness of films was measure using reflectance spectra shown in figure 4. The plot of  $(\alpha h\nu)^2$  against  $h\nu$  are shown in figure 5. By extrapolating the linear part of the plot to  $\alpha = 0$ , optical band gap was estimated and it is 3.22 eV for the film deposited at 100 ml.

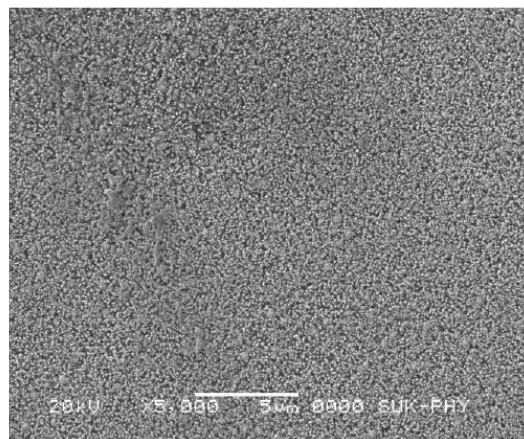


**Figure 2 : Scanning electron micrograph of ZnO thin film at 0.2M, 400°C.**

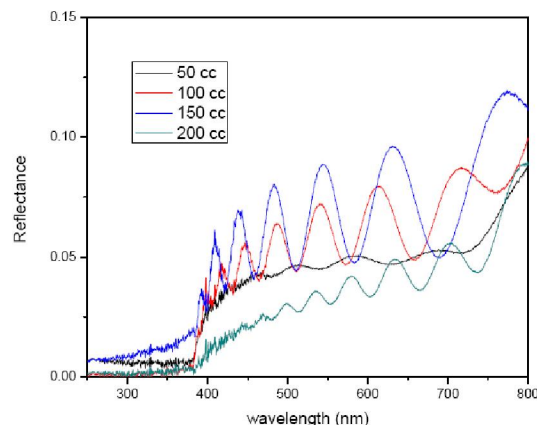


**Figure 3 : Reflectance spectra of ZnO thin film deposited at temperature of 400°C**

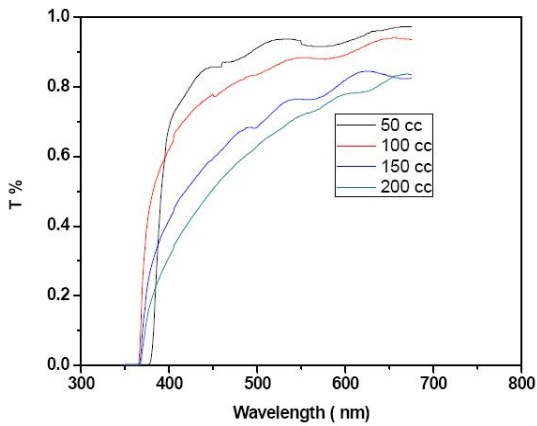


Figure 4 : Transmittance spectra of ZnO thin film deposited at temperature of 400°C

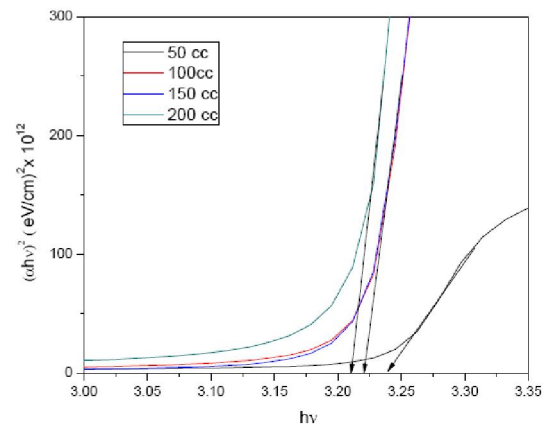


Figure 5 : Plot of  $(\alpha hv)^2$  vs  $h\nu$  of typical ZnO thin film deposited at temperature of 400°C

TABLE 1 : Quantity dependent parameters of ZnO thin films.

Quantity of sprayed Solution (cc)	Thickness (nm)	Crystallite size (nm)	Reflectance Coeff.at 555 nm	Transmittance Coeff.at 555 nm	Direct BandGap (eV)	Resistivity ( $\Omega/cm$ )
50	57	52.86	0.045	0.916	3.23	1.589
100	790	46.98	0.068	0.882	3.22	1.279
150	835	38.43	0.088	0.760	3.22	$6.15 \times 10^{-1}$
200	1208	38.43	0.033	0.720	3.21	$5.85 \times 10^{-1}$

### Photoelectrohydrolysis of starch

Figure 6 shows the typical visible spectra as function of time of starch iodine complex. A decrease in absorption at round 583 nm peaks is observed as time increases. Also absorption peak is shifted towards higher wavelength, which indicates presence of maltose and glucose. A plot of the maximum absorbance verses time represents evolution of the process (Starch + Photoelectrocatalytic process  $\rightarrow$  Modified starch + maltose + glucose +  $CO_2 \uparrow$ ). Figure 7 shows that blue colour of starch - iodine complex decreases as function of time indicates degradation of starch during photoelectrocatalysis. Percentage of degradation rep-

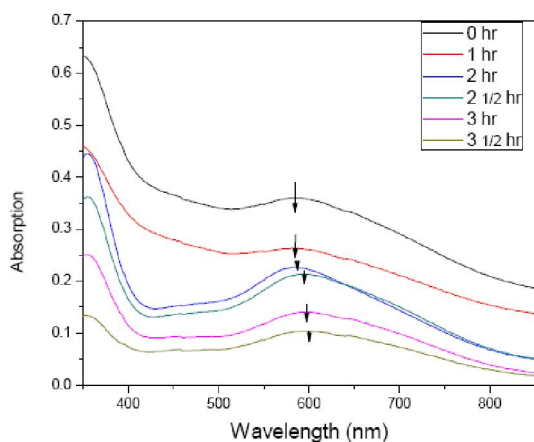


Figure 6 : Visible spectra of starch-iodine complex



Figure 7 : Colour of starch-iodine complex samples

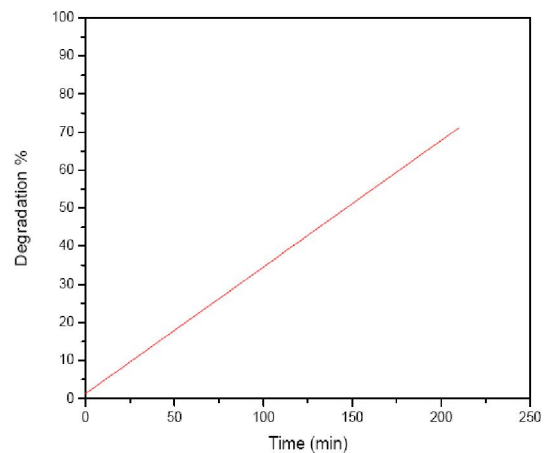


Figure 8 : Percentage of degradation of starch with respect to time.

## Full Paper

resented by figure 8 and it shows that 72.7 % of original starch degraded within 210 min. In order to quantify the hydrolysis of starch the absorption at 583 nm was plotted as function of time (figure 8). The reaction kinetics is represented by the following equation

$$Y = Y_0 + A_1 \exp(-x/t) \quad (3)$$

Figure 9 shows typical Raman spectra for the starch samples of unhydrolyzed and hydrolyzed starch; the main vibrational bands are listed in TABLE 2, together with their respective tentative assignments, based on comparison with literature data<sup>[18]</sup>. The region at 2,907 cm<sup>-1</sup> is related to the symmetrical and antisymmetrical CH stretching. The intensity changes in 3,135 and 3,235 cm<sup>-1</sup> range can be mainly attributed to the variations in the amount of amylose and amylopectin present in starches. On the other hand, the region between 1,461 and 1,050 cm<sup>-1</sup> is rich in structural information; the Raman spectra of carbohydrates present several vibrational features in this region. Most of the bands are due to coupled vibrations involving hydrogen atoms; for instance, one can see a feature at 1,461 cm<sup>-1</sup>, which corresponds to CH, CH<sub>2</sub>, and COH deformations. In the region between 1,380 and 1,400 cm<sup>-1</sup> one can observe the coupling of the CCH and COH deformation modes, whereas in the region between 1,340 and 1,200 cm<sup>-1</sup> bands containing the contributions of several vibrational modes are observed, such as CO and CC stretching and CCH, COH, and CCH deformations.<sup>[19]</sup>,  $\alpha$ -1,4 glycosidic linkages can be observed as strong Raman bands in the 920-960-cm<sup>-1</sup> region, and thus the band observed at 940 cm<sup>-1</sup> was assigned to the amylose  $\alpha$ -1,4 glycosidic linkage. The very intense Raman band at 478-479 cm<sup>-1</sup> has been used as a marker to identify the presence of amylose and amylopectin in starch. The raman spectra of both starch exhibited some (479cm<sup>-1</sup>, 1265 cm<sup>-1</sup>, 1341 cm<sup>-1</sup>, 1461 cm<sup>-1</sup>, and 2911 cm<sup>-1</sup>) identical bands, because those bands originated mainly vibrational modes of amylose and amylopectine. However, some peaks (941 cm<sup>-1</sup> to 936 cm<sup>-1</sup>, 1053 cm<sup>-1</sup> to 1050 cm<sup>-1</sup>, 1126 cm<sup>-1</sup> to 1125 cm<sup>-1</sup>, 1380 cm<sup>-1</sup> to 1382 cm<sup>-1</sup>) shifts occur relative to pure starch. The most significant difference in raman spectra (figure 9) observed in the region 1770 cm<sup>-1</sup> to 2267 cm<sup>-1</sup> and 3135 cm<sup>-1</sup> to 3235 cm<sup>-1</sup> might due to  $\delta$ (O-H) bend.

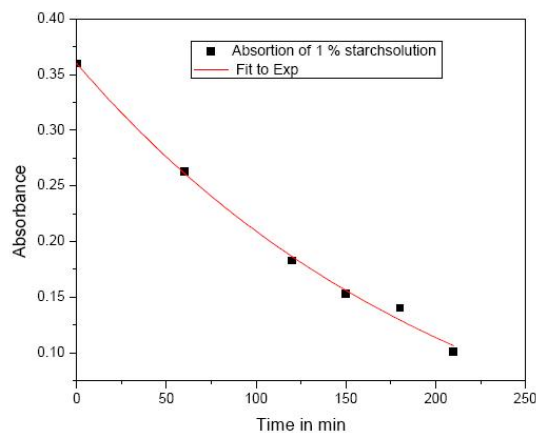
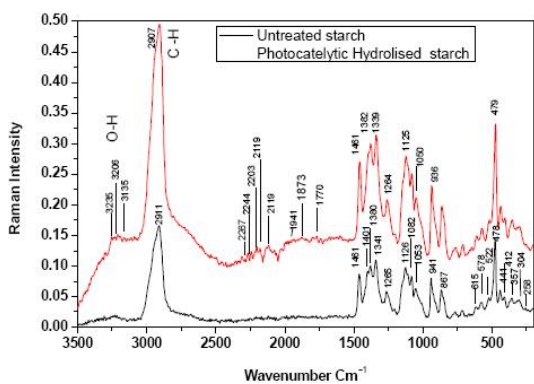


Figure 9 : Absorption at 583 nm with respect to time

TABLE 2 : Raman wavenumbers and their respective tentative assignments based on literature data<sup>[19]</sup>

Unhydrolysed Starch	Hydrolysed Starch	Assignment
258	-	
304	-	
357	-	
412	-	$\delta$ (C-C-O)+ $\delta$ (C-C-C)
441	-	$\delta$ (C-C-O)+ $\delta$ (C-C-C)
478	479	$\delta$ (C-C-C)+ $\tau$ (C-O)
522	-	$\delta$ (C-C-C)+ $\tau$ (C-O)
578	-	$\delta$ (C-C-C)+ $\tau$ (C-O)
615	-	$\delta$ (C-C-O)
867	-	$\delta$ (C-C-H)+ $\delta$ (C-O-C)
941	936	$\delta$ (C-O-C)+ $\delta$ (C-O-H)+ $\nu$ (C-O)
1053	1050	$\nu$ (C-O)+ $\nu$ (C-C)+ $\delta$ (C-O-H)
1082	-	$\nu$ (C-O)+ $\nu$ (C-C)+ $\delta$ (C-O-H)
1126	1125	$\nu$ (C-O)+ $\nu$ (C-C)+ $\delta$ (C-O-H)
1265	1264	$\nu$ (C-O)+ $\nu$ (C-C)+ $\delta$ (C-O-H)
1341	1339	$\nu$ (C-O); $\delta$ (C-O-H)
1380	1382	$\delta$ (C-O-H)
1401	-	$\delta$ (C-C-H)
1461	1461	$\delta$ (CH)+ $\delta$ (CH <sub>2</sub> )+ $\delta$ (C-O-H)
-	1770	$\delta$ (O-H) bend
-	1873	$\delta$ (O-H) bend
-	1941	$\delta$ (O-H) bend
-	2129	$\delta$ (O-H) bend
-	2179	$\delta$ (O-H) bend
-	2203	$\delta$ (O-H) bend
-	2244	$\delta$ (O-H) bend
-	2267	$\delta$ (O-H) bend
2907	2911	$\nu$ (C-H)
-	3135	$\delta$ (O-H) stretch
-	3206	$\delta$ (O-H) stretch
-	3235	$\delta$ (O-H) stretch



**Figure 10 : Raman spectra for unhydrolyzed and hydrolyzed starch**

To determine the hydrolysis of starch, collected solution was checked for the presence of starch monomers by DNSA method<sup>[20]</sup>. Solution was found to contain  $60\mu\text{g ml}^{-1}$  of glucose and  $100\mu\text{g ml}^{-1}$  of maltose. From this we can conclude that starch was hydrolyzed. However the exact mechanism of photoelectrocatalytic hydrolysis is unknown and needs further investigation.

## CONCLUSION

All the films are polycrystalline with hexagonal wurtzite structure, with c- axis growth (002) perpendicular to substrate surface. The film deposited at sprayed quantity 100 cc is suitable for photoelectrocatalytic hydrolysis of starch. Modified starch may be used for industrial use. For controlled hydrolysis of starch more further investigation is required.

## REFERENCES

- [1] G.Kenanakis, Z.Giannakoundakis, D.Vernardou, C.Savvakis, N.Katsarakis; *Catalysis Today*, **151**, 34-38 (2010).
- [2] L.Schmidt Mende, J.L.Macmanus-Driscoll; *Matter Today*, **10**(5), 40 (2007).
- [3] S.Sakthivel, B.Neppolian, M.V.Shankar, B.Arabindoo, M.Palanichamy, V.Murugesan; *Sol.Energy Mater. Sol.Cells*, **77**, 65 (2003).
- [4] P.S.Shinde, S.B.Sadale, P.S.Patil, P.N.Bhosale, A.Bruger, M.Neumann-Spallart, C.H.Bhosale; *Sol.Energy Mater.Sol.Cells*, **92**, 283-290 (2008).
- [5] P.S.Shinde, S.B.Sadale, P.S.Patil, P.N.Bhosale, A.Bruger, M.Neumann-Spallart, C.H.Bhosale; *Appl.Cat.B: Environ.*, **89**, 288-294 (2009).
- [6] F.Peng, H.Wang, H.Yu; *S.Chem.Mater Res.Bull.*, **41**, 2123 (2006).
- [7] F.Xu, G.H.Du, M.Halasa, B.-I.Su; *Chem.Phys.Lett.*, **426**, 129 (2006).
- [8] I.M.Lipatova, N.V.Losev, A.A.Yuseva; *Russian J.Appl.Chemistry*, **76**, 1532-1537 (2006).
- [9] K.Tamilarasan, R.Ashok, S.Abinandan, M.Dharmendira Kumar; *International Journal of Biotechnology and Biochemistry*, **6**, 841-850 (2010).
- [10] P.Bernazzani, H.Krishna Reddy Pandi, V.Krishna Peyyavula; *J.Chem-Bio-Chem and Molecular Biology*, 4008, 2, 1.
- [11] B.Bej, R.K.Basu, S.N.Ash; *J.Scientific and Industrial Res.*, **67**, 295-298 (2008).
- [12] M.E.Vander, A.J.Vander Goot, R.M.Boom; *Biotechnology Progress*, **21**, 598-602 (2005).
- [13] J.Tovar, S.G.Sayago-Ayerdi, C.Penalver, O.Paredes-Lopez, L.A.Bello-Perez; *Cereal Chem.*, **80**, 533-535 (2003).
- [14] H.Gomez, L.Mdela; *Mater Sci.Eng.B*, **134**, 20 (2006).
- [15] M.Caglar, Y.Caglar, S.Ilican; *J.Photoelectronics and Adv.Mater.*, **8**, 1410-1413 (2006).
- [16] Re K.Kayal, Mehmet Ar, S.Mustafa Ozta, Metin Bedir, Funda Aksoy; *Chin.PPhys.Lett.*, **26**(1), 017106 (2009).
- [17] U.Ayer; *Thin Solid Films*, **515**, 3448 (2007).
- [18] M.R.Almeida, R.S.Alves, B.L.Larra, N.R.Stephani, R.J.Poppi, F.C.Luiz De Oliveira; *Anal.Biomol. Chem.*, **397**, 2693-2701 (2010).
- [19] R.Kize, J.Irudayaraj; *J.Agricultural and Food Chemistry*, **9**, American Chemical Society, (2006).
- [20] David R.Lide; *Handbook of Chemistry and Physics*, 87<sup>th</sup> Edition, Boca Raton, FL: CRC Press, 3-318 (1998).